

## A Novel Approach of Image Enhancement using Steganographic Data Embedding and JPEG Scheme

Isao FURUKAWA\* and Junji SUZUKI\*\*

(Received Oct. 30, 2013)

### Abstract

We propose a new image enhancement method for JPEG images on the Internet that a sender who has high resolution images embeds enhancement codes for representing high frequency DCT coefficients into low frequency DCT coefficients, and receivers recover either low resolution JPEG coded images by using conventional JPEG decoder or high resolution images by using code extraction from low frequency DCT coefficients. This image transmission method can be thought as so called steganographic communication in case that these enhancement codes are kept secret. In order to implement the steganographic image communication, after the DCT size is extended from  $8 \times 8$  to  $16 \times 16$ , SNRs are measured for images not only with setting all high frequency coefficients greater than  $8 \times 8$  size to zeros, then processing IDCT of  $16 \times 16$  size, but also with processing IDCT of  $8 \times 8$  size. A scanning method for high frequency DCT coefficients is also proposed. The simulation experiments show the amount of enhancement codes for recovering quantized high frequency DCT coefficients and SNRs without embedding enhancement codes into low frequency DCT coefficients.

**Key Words:** image communication, steganography, image enhancement, JPEG compression, DCT, entropy coding

### 1. INTRODUCTION

A high resolution image can be obtained by adding high frequency components to a low resolution image with some restricted bandwidth. On the other hand, an image enhancement method called super resolution (SR) is also used, if the high frequency components are estimated from only low resolution images without using high frequency signal information [1]. This problem is essentially ill-posed one and the precise recovering is impossible [2], because the estimated high frequency components are beyond the maximum frequency that is restricted by the sampling theorem. A reasonable reconstruction of the high frequency components needs a priori knowledge about the original image. For example, missing

high frequency components are estimated by Bayesian estimation using multiple image frames of the same scene [3]. As mentioned above, conventional image enhancement technologies such as SR only estimate missing signals, so that these have restricted properties that rely on edge enhancement, nonlinear filtering, spline functional interpolation, and so on when a single image frame is available, though these have some advantages when several images are available.

A basic idea of communications with steganographic information-embedded image enhancement scheme is that the high frequency components are embedded in the low frequency components in the encoder, and then the embedded components are utilized to recover enhanced images in the decoder. For

---

\* Department of Computer Science, Faculty of Applied Information Science, Hiroshima Institute of Technology

\*\* School of Information Science and Technology, Aichi Prefectural University

example, an steganographic image compression method that is premised on using JPEG as the underlying image coding method enables the parties who know the secret can recover high resolution images exclusively, and the public people who do not know the secret can only recover low resolution images using a conventional JPEG decoder. This means that the steganographic image compression method have a compatibility with the existing systems, if the output bit stream of the encoder is conforming to the JPEG standard. Moreover it may not seem to be a covert communication at a first glance. Of course, there are many steganalysis methods that investigate the outlier of the encoder output codes from the normal JPEG encoder bit stream, but it is not often done and may not be suspicious.

Another application is for a business model that high resolution images, such as 4K, can be incorporated in the existing HDTV broadcasting system by embedding the high frequency components in the low frequency signal. In this scenario, users who have 4K TV can view 4K image contents with additional payment to extract and decrypt the embedded components.

In order to implement the steganographic image enhancement system, we have to study the frequency characteristics of DCT viewed as a filter bank, embedding method of high frequency component into low frequency signal, and human visual sensitivity against quality degradation by information embedding. This paper discusses basic experimental results toward the implementation of the steganographic image enhancement communication. First of all, a fundamental framework to design steganographic information embedding method based on the JPEG standard is described in Section 2. The simulation conditions for the experiments are presented in Section 3. The simulation results are demonstrated in Section 4, and conclusions are given in Section 5.

## 2. BASIC CONFIGURATIONS

### 2.1 Encoder and decoder systems

This system assumes a couple of special encoder and decoder, and conventional decoders placed on the Internet. These encoder and decoders have the following functions.

- (a) Special encoder: Original images with  $2N \times 2N$  pixels are first transformed by  $16 \times 16$  DCT, and

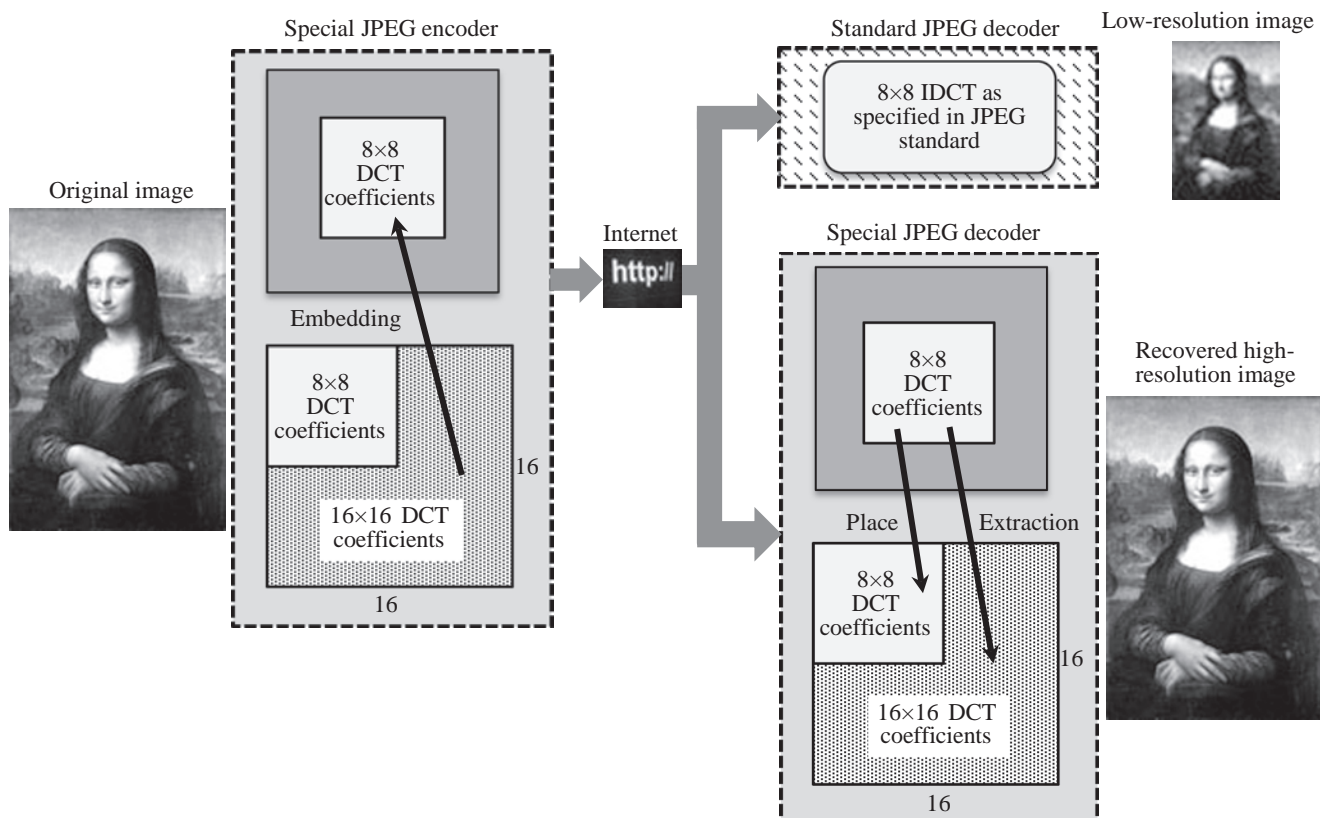


Fig. 1 Notion of image enhancement with JPEG and steganographic data embedding.

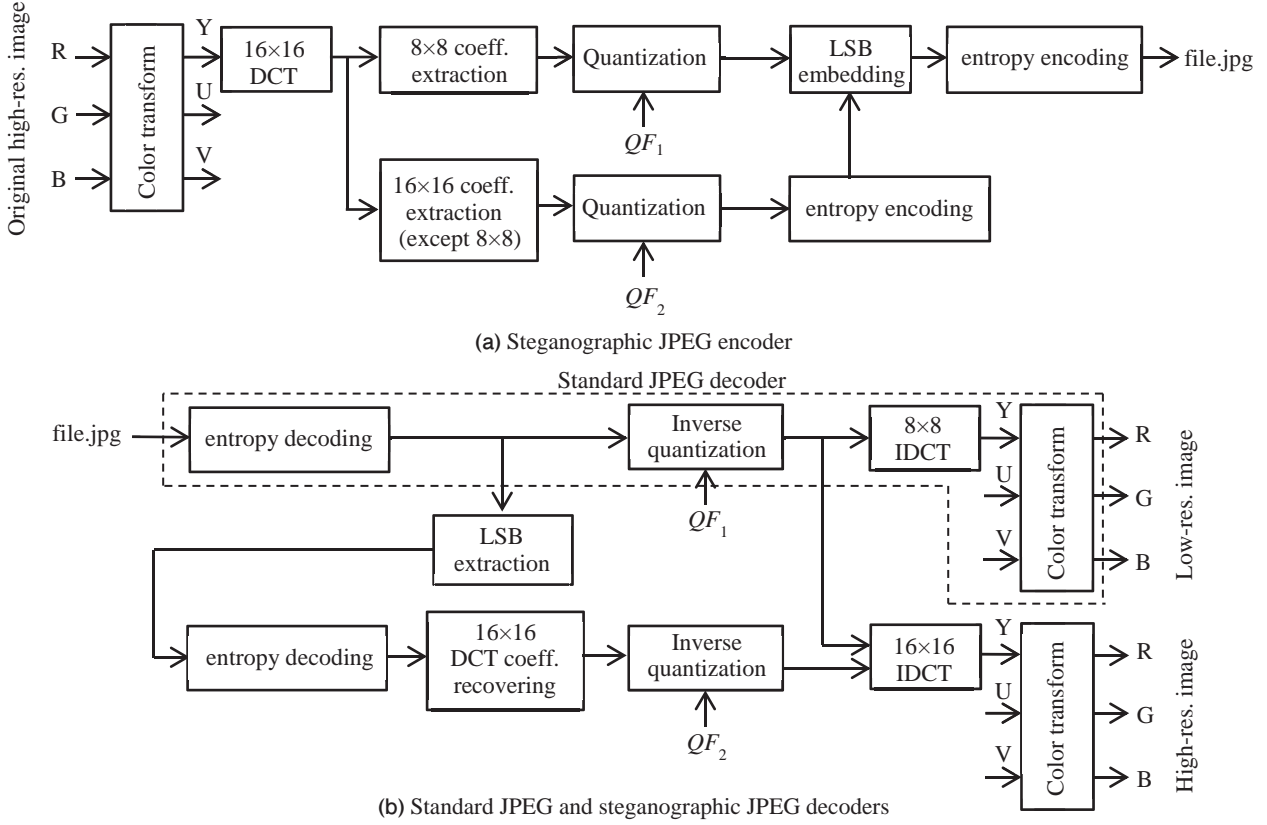


Fig. 2 Configurations of steganographic JPEG encoder/decoder and standard JPEG decoder.

then the codes for the quantized high frequency DCT coefficients other than  $8 \times 8$  coefficients are embedded in the LSBs of  $8 \times 8$  quantized low frequency DCT coefficients. The  $8 \times 8$  DCT coefficients are encoded using conventional JPEG entropy encoder. The output of the special encoder is conformed to the JPEG standard.

- (b) Standard decoder: It receives a JPEG bit stream embedded high frequency components in  $8 \times 8$  DCT coefficients, and decodes it to obtain a decoded image with  $N \times N$ -pixel resolution by conventional JPEG decoding procedure.
- (c) Special decoder: It receives a JPEG bit stream embedded high frequency components in  $8 \times 8$  DCT coefficients, and extract the quantized high frequency DCT coefficients to obtain  $16 \times 16$  DCT coefficients, then a  $2N \times 2N$ -pixel resolution images are recovered by  $16 \times 16$  IDCT.

One example for the encoder and the decoders' arrangement is shown in Figure 1. The special encoder described above outputs a bit stream that has apparently different characteristics from that of the conventional JPEG encoder (e.g., the file size from

the special encoder will be larger than that from the conventional JPEG encoder), so that the steganographic embedding may be identified using various statistical analysis. If the image content is not so valuable, no security guard will be necessary. Otherwise, it can be protected using secure methods such as encryption.

Figure 2 shows the configurations of the steganographic JPEG encoder/decoder and the standard JPEG decoder to implement the functions depicted in Figure 1. The individual functions are described below.

## 2.2 DCT/IDCT as filter bank system

### 2.2.1 $N$ -point DCT and $N$ -point IDCT

Let us consider a frequency characteristic of one dimensional DCT/IDCT system that the  $N$ -point IDCT is performed after setting zeros of the higher frequency coefficients other than lower  $L$ -point coefficients of the  $N$ -point DCT. This DCT/IDCT system is shown in Figure 3. The output of the system,  $y(n)$ , that the output of the  $N$ -point DCT,  $X(n)$ , is restricted up to lower  $L$  points can be shown as follows by  $N$ -

point DCT/IDCT formula, which is same as that used in the JPEG standard.

$$y(n) = \frac{2}{N} \sum_{m=0}^{N-1} x(m) \left[ \sum_{k=0}^{L-1} \cos \frac{(2m+1)k\pi}{2N} \cos \frac{(2n+1)k\pi}{2N} - \frac{1}{2} \right], \quad (1)$$

where  $n$  is an integer,  $n = 0, 1, \dots, N-1$ . Then, as the coefficient of  $x(m)$  is a constant if  $n$  and  $m$  are determined, it is written by

$$h_{n,m} = \frac{2}{N} \left[ \sum_{k=0}^{L-1} \cos \frac{(2m+1)k\pi}{2N} \cos \frac{(2n+1)k\pi}{2N} - \frac{1}{2} \right], \quad (2)$$

and we get the following relationship from Eq. (1).

$$y(n) = \sum_{m=0}^{N-1} h_{n,m} x(m), \quad n = 0, \dots, N-1. \quad (3)$$

Actually, Eq. (3) is constructed with  $N$  equations concerning with  $y(n)$ ,  $n = 0, \dots, N-1$ .

$$\left. \begin{aligned} y(0) &= h_{0,0}x(0) + h_{0,1}x(1) + \dots + h_{0,N-1}x(N-1), \\ y(1) &= h_{1,0}x(0) + h_{1,1}x(1) + \dots + h_{1,N-1}x(N-1), \\ &\dots \\ y(N-1) &= h_{N-1,0}x(0) + h_{N-1,1}x(1) + \dots + h_{N-1,N-1}x(N-1). \end{aligned} \right\} \quad (4)$$

This set of equations can be seen as the following  $N$  FIR digital filters.

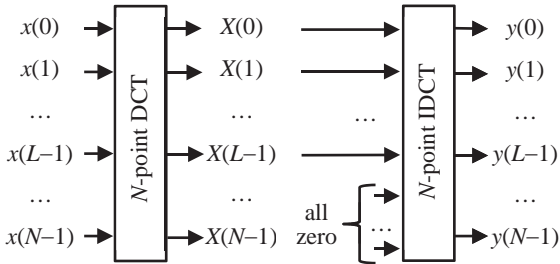


Fig. 3  $N$ -point DCT/ $N$ -point IDCT system with only  $L$ -point coefficients.

$$\left. \begin{aligned} y_1(n) &= h_{0,0}x(n) + h_{0,1}x(n+1) + \dots + h_{0,N-1}x(n+N-1), \\ y_2(n) &= h_{1,0}x(n-1) + h_{1,1}x(n) + \dots + h_{1,N-1}x(n+N-2), \\ &\dots \\ y_{N-1}(n) &= h_{N-1,0}x(n-N+1) + h_{N-1,1}x(n-N+2) + \dots + h_{N-1,N-1}x(n). \end{aligned} \right\} \quad (5)$$

By Z-transforming, we get

$$\left. \begin{aligned} Y_1(z) &= (h_{0,0} + h_{0,1}z^1 + \dots + h_{0,N-1}z^{N-1})X(z), \\ Y_2(z) &= (h_{1,0}z^{-1} + h_{1,1} + \dots + h_{1,N-1}z^{N-2})X(z), \\ &\dots \\ Y_{N-1}(z) &= (h_{N-1,0}z^{-(N-1)} + h_{N-1,1}z^{-(N-2)} + \dots + h_{N-1,N-1})X(z), \end{aligned} \right\} \quad (6)$$

therefore, if we define  $H_n(z) = Y_n(z)/X(z)$ ,  $n = 0, \dots, N-1$ , as a transfer function of the filter bank system, this can be written as

$$\left. \begin{aligned} H_1(z) &= h_{0,0} + h_{0,1}z^1 + \dots + h_{0,N-1}z^{N-1}, \\ H_2(z) &= h_{1,0}z^{-1} + h_{1,1} + \dots + h_{1,N-1}z^{N-2}, \\ &\dots \\ H_{N-1}(z) &= h_{N-1,0}z^{-(N-1)} + h_{N-1,1}z^{-(N-2)} + \dots + h_{N-1,N-1}. \end{aligned} \right\} \quad (7)$$

As a result, we get the transfer function of the filter bank system as follows.

$$H_n(z) = \sum_{m=0}^{N-1} h_{n,m} z^{m-n}, \quad n = 0, \dots, N-1. \quad (8)$$

The outputs of the FIR digital filter would not been seen as the summed result of each digital filters when they are constructed in parallel, because the final output signals of the system are not summed to obtain  $y(n)$  (i.e.,  $N$  pieces of  $y(n)$  signals themselves are the output of the system). Therefore,  $H(z) \neq \sum_n H_n(z)$ , where  $H(z)$  is an overall transfer function of the filter bank system. We assume instead that the expected transfer function is obtained when the outputs of these  $N$  digital filters are observed as an average. That is, we expect the spectrum amplitude of the overall transfer function  $|H(z)|$  as follows, which is derived from the digital filters of  $N$ -point DCT/ $N$ -point IDCT system.

$$|H(z)| = \frac{1}{N} \sum_{n=0}^{N-1} |H_n(z)|. \quad (9)$$

It is obvious that the overall transfer function is equal to 1 in case of  $L = N$ .

Figure 4 shows  $|H_n(z)|$  ( $n = 0, 1, \dots, 15$ ) and  $|H(z)|$  with  $N = 16$  and  $L = 8$ , while Figure 5 shows  $|H(z)|$  with  $L = 8, 9, \dots, 16$ . These results show that the filter bank system has a low pass characteristic, and the attenuation magnitude of the stop band frequency is about 15 (dB).

### 2.2.2 $N$ -point DCT and $L$ -point IDCT ( $L \leq N$ )

Let us consider a frequency characteristic of one dimensional DCT/IDCT system that the  $L$ -point IDCT ( $L \leq N$ ) is performed after discarding the higher frequency coefficients other than lower  $L$ -point coefficients of the  $N$ -point DCT. This DCT/IDCT system is shown in Figure 6. In this case, the gain of the output signal,  $y(n)$ , resulted from the  $L$ -point IDCT is multiplied by  $\sqrt{L/N}$ , because the order of the base cosine function is changed. Therefore, the output of the system,  $y(n)$ , that the higher frequency coefficients of the  $N$ -point DCT,  $X(n)$ , are discarded can be

shown as follows by  $N$ -point DCT/ $L$ -point IDCT formula, which is same as that used in the JPEG standard.

$$y(n) = \frac{2}{N} \sum_{m=0}^{N-1} x(m) \left[ \sum_{k=0}^{L-1} \cos \frac{(2m+1)k\pi}{2N} \cos \frac{(2n+1)k\pi}{2L} - \frac{1}{2} \right]. \quad (10)$$

As discussed in 2.2.1, the coefficient of  $x(m)$  is a constant if  $n$  and  $m$  are determined, and it is written by

$$g_{n,m} = \frac{2}{N} \left[ \sum_{k=0}^{L-1} \cos \frac{(2m+1)k\pi}{2N} \cos \frac{(2n+1)k\pi}{2L} - \frac{1}{2} \right], \quad (11)$$

and we get the following relationship from Eq. (10).

$$y(n) = \sum_{m=0}^{N-1} g_{n,m} x(m), \quad n = 0, \dots, L-1. \quad (12)$$

Actually, Eq. (12) is constructed with  $N$  equations concerning with  $y(n)$ ,  $n = 0, \dots, N-1$ .

$$\left. \begin{aligned} y(0) &= g_{0,0}x(0) + g_{0,1}x(1) + \dots + g_{0,N-1}x(N-1), \\ y(1) &= g_{1,0}x(0) + g_{1,1}x(1) + \dots + g_{1,N-1}x(N-1), \\ &\dots \\ y(L-1) &= g_{L-1,0}x(0) + g_{L-1,1}x(1) + \dots + g_{L-1,N-1}x(N-1). \end{aligned} \right\} \quad (13)$$

This set of equations can be seen as the following  $N$  FIR digital filters.

$$\left. \begin{aligned} y_1(n) &= g_{0,0}x(n) + g_{0,1}x(n+1) + \dots + g_{0,N-1}x(n+N-1), \\ y_2(n) &= g_{1,0}x(n-1) + g_{1,1}x(n) + \dots + g_{1,N-1}x(n+N-2), \\ &\dots \\ y_{L-1}(n) &= g_{L-1,0}x(n-N+1) + g_{L-1,1}x(n-N+2) + \dots + g_{L-1,N-1}x(n). \end{aligned} \right\} \quad (14)$$

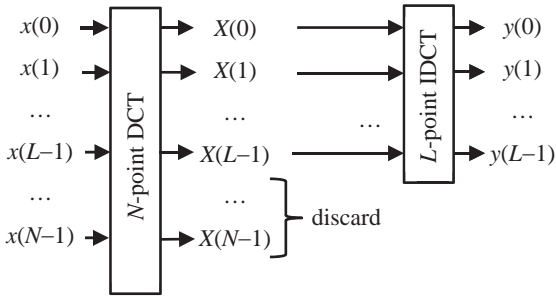


Fig. 6  $N$ -point DCT/ $L$ -point IDCT system with only  $L$ -point coefficients.

By Z-transforming, we get

$$\left. \begin{aligned} Y_1(z) &= (g_{0,0} + g_{0,1}z^1 + \dots + g_{0,N-1}z^{N-1})X(z), \\ Y_2(z) &= (g_{1,0}z^{-1} + g_{1,1} + \dots + g_{1,N-1}z^{N-2})X(z), \\ &\dots \\ Y_{L-1}(z) &= (g_{L-1,0}z^{-(N-1)} + g_{L-1,1}z^{-(N-2)} + \dots + g_{L-1,N-1})X(z). \end{aligned} \right\} \quad (15)$$

therefore, if we define  $G_n(z) = Y_n(z)/X(z)$ ,  $n = 0, \dots, N-1$ , as a transfer function of the filter bank system, this can be written as

$$\left. \begin{aligned} G_1(z) &= g_{0,0} + g_{0,1}z^1 + \dots + g_{0,N-1}z^{N-1}, \\ G_2(z) &= g_{1,0}z^{-1} + g_{1,1} + \dots + g_{1,N-1}z^{N-2}, \\ &\dots \\ G_{L-1}(z) &= g_{L-1,0}z^{-(N-1)} + g_{L-1,1}z^{-(N-2)} + \dots + g_{L-1,N-1}. \end{aligned} \right\} \quad (16)$$

As a result, we get the transfer function of the filter bank system as follows.

$$G_n(z) = \sum_{m=0}^{N-1} g_{n,m} z^{m-n}, \quad n = 0, \dots, L-1. \quad (17)$$

If we assume that the expected transfer function is obtained when the outputs of these  $N$  digital filters are observed as an average as discussed in 2.2.1, the transfer function  $|G(z)|$  is expressed as follows, which is derived from the digital filters of  $N$ -point DCT/ $L$ -point IDCT system.

$$|G(z)| = \frac{1}{L} \sum_{n=0}^{L-1} |G_n(z)|. \quad (18)$$

It is obvious that the overall transfer function is equal to 1 in case of  $L = N$ .

Figure 7 shows  $|G_n(z)|$  ( $n = 0, 1, \dots, 7$ ) and  $|G(z)|$  with  $N = 16$  and  $L = 8$ , while Figure 8 shows  $|G(z)|$  with  $L = 8, 9, \dots, 16$ . These results show that the filter bank system has a low pass characteristic, and the attenuation magnitude of the stop band frequency is around 10 to 15 (dB).

### 2.3 Scanning of higher frequency DCT coefficients and its code representation

The special encoder is divided into two parts: one is for encoding  $8 \times 8$  DCT coefficients within  $16 \times 16$  DCT coefficients, the other is for encoding  $16 \times 16$  DCT coefficients other than lower  $8 \times 8$  DCT coefficients. For extracting the latter higher frequency DCT coefficients, we employ a scanning method with inverse L-shaped pattern as shown in Figure 9. In this case, the numbers of scanned quantized DCT coefficients are,

$$\left. \begin{aligned} \text{first scan: } &9 + 9 - 1 = 17 \text{ coefficients,} \\ \text{second scan: } &10 + 10 - 1 = 19 \text{ coefficients,} \\ \text{third scan: } &11 + 11 - 1 = 21 \text{ coefficients,} \\ &\dots \\ \text{8-th scan: } &16 + 16 - 1 = 31 \text{ coefficients,} \end{aligned} \right\}$$

hence, the total number of scanned coefficients is  $17 + 19 + 21 \dots + 31 = 192$ . The encoded data with run-length Huffman encoding method are embedded in  $8 \times 8 = 64$  lower frequency DCT coefficients.

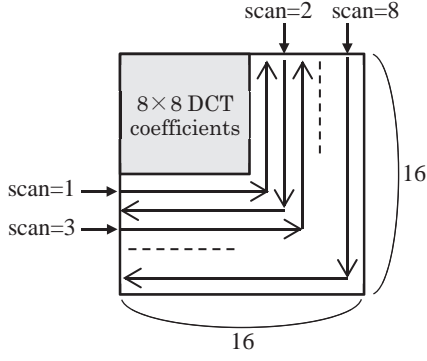


Fig 9. Scan pattern for higher frequency DCT coefficients

As shown in Figure 2, it is possible to define that the quality factors ( $QF$ s) for lower  $8 \times 8$  DCT coefficients and higher  $16 \times 16$  DCT coefficients other than  $8 \times 8$  have different values of  $QF_1$  and  $QF_2$ , respectively. The quantization step size  $A_i$  is computed as follows using the quality factor,  $QF \in \{1, 2, \dots, 99\}$  when the default quantization step size is  $B_i$ .

$$A_i = \left\lfloor \frac{B_i \cdot S + 50}{100} \right\rfloor, \quad (19)$$

where

$$S = \begin{cases} 200 - 2QF & \text{for } QF \geq 50, \\ 5000 / QF & \text{for } QF \leq 50. \end{cases} \quad (20)$$

If  $QF = 50$ , then the quantization is set as the default value. The quality factors of  $QF > 50$  and  $QF < 50$  give high quality quantization (low compression rate) and low quality quantization (high compression rate), respectively. For example,

• if  $QF = 50$ ,

$$A_i = \left\lfloor \frac{B_i \cdot 100 + 50}{100} \right\rfloor = \left\lfloor B_i + \frac{1}{2} \right\rfloor = B_i,$$

• else if  $99 \geq QF > 50$ ,

$$A_i = \left\lfloor \frac{B_i \cdot (200 - 2QF) + 50}{100} \right\rfloor = \left\lfloor B_i \left( 2 - \frac{QF}{50} \right) + \frac{1}{2} \right\rfloor,$$

• else if  $1 \leq QF < 50$ ,

$$A_i = \left\lfloor \frac{B_i \cdot (5000/QF) + 50}{100} \right\rfloor = \left\lfloor B_i \frac{50}{QF} + \frac{1}{2} \right\rfloor.$$

In order to make the encoding of the enhancement data easy, we use default run-length Huffman codes for zigzag scanning of  $8 \times 8$  quantized DCT coefficients for luminance and chrominance components. Here, if all the coefficients in the higher frequency domain is zero, then a specific code of EOB (end of block) is assigned to express the state, so that the enhancement code is 4-bit “1010” for the luminance component and 2-bit “00” for the chrominance

component in such a case, and these codes give minimum code length. Of course, the amount of the enhancement codes depends on the quality factor for the higher frequency DCT coefficients as described above.

### 3. EXPERIMENT CONDITIONS

Now, we explain the subjects that should be clarified by the simulation experiments.

- (1) The quality factor for the  $8 \times 8$  DCT coefficients that makes the quantization noise invisible when  $8 \times 8$  DCT coefficients are inverse transformed with  $16 \times 16$  IDCT.
- (2) As discussed in 2.2.1 and 2.2.2, DCT/IDCT system can be viewed as a filter bank and the attenuation magnitude in the stop band frequency is around 10 to 15 (dB). This attenuation magnitude may be too small to make the ringing artifacts invisible. In order to prevent the artifacts, we employ two approaches: The first is to clarify the number of scans to prevent the ringing artifacts when the number of scans of the higher DCT coefficients becomes  $9 \times 9$ ,  $10 \times 10$ , ...,  $16 \times 16$  (in this case, the parameter is the quality factor for lower frequency DCT coefficient quantization). The second is to clarify the quality factor to prevent the ringing artifact when all the  $16 \times 16$  DCT coefficients are used (in this case, the parameter is the quality factor for the higher frequency DCT coefficient quantization).
- (3) In case of (2), how much the amount of the enhancement codes compared with the resulting JPEG entropy codes is, and how much the rate described above decreases when the quality factor of the lower frequency DCT coefficients increases. In other words, what is the characteristic of the payload for the enhancement codes?
- (4) Do the results from (1) through (3) change with different image contents and the pixel resolution of original images?

In order to consider the above mentioned subjects, we divide the experiment into three phases, i.e., phases I to III. Note that the actual embedding of the enhancement codes into the lower frequency DCT coefficients is not implemented, because we treat it as a further study in conjunction with a subjective

test. The experiment phases I to III are as follows:

- I. The SNRs for which reduced-size JPEG coded image and original-size JPEG coded image without image enhancement (i.e., scan = 0) are measured with various quality factors of the lower frequency DCT coefficient quantization. These SNRs include three measurements:  $\text{SNR}_{\text{lowres}}$  that is computed using reduced-size JPEG coded image and  $16 \times 16$  DCT/ $8 \times 8$  IDCT image as a reference,  $\text{SNR}_{\text{lowpass}}$  that is computed using original-size JPEG coded image with scan = 0 and original high resolution image as a reference, and SNR that is computed using only low-passed original-size  $16 \times 16$  DCT/ $16 \times 16$  IDCT with zero higher frequency and original high resolution image as a reference. The compression ratio of the reduced-size JPEG coding is also measured. These measurements are applied to the three chrominance formats of 4:4:4, 4:2:2, and 4:1:1. A simple subjective test is performed to obtain a guideline needed for the quality factor of the lower frequency DCT coefficients in case of scan = 0 (the quality factors,  $QF_1$ , are selected as 40, 45, 50, 55, ..., 90, 95 with step of 5).
- II. In addition to the conditions of experiment phase I, the quality factor,  $QF_1$ , needed to make the artifacts invisible should be confirmed when the enhancement codes are used to recover the original-size JPEG encoded image. In order to obtain a fundamental property, the amount of enhancement codes is measured with various combinations of the quality factor of the higher frequency DCT coefficients,  $QF_2$ , and the number of scans. More precisely, An average, maximum, and minimum amount of enhancement codes per block ( $16 \times 16$  region) for a combinations of scan = 1, 2, ..., 8 and  $QF_2 = 40, 45, 50, 55, \dots, 90, 95$  with step of 5. In this experiment,  $QF_1$  is irrelevant to the results
- III. The steganographic data embedding is equivalent to adding quantization distortion to  $8 \times 8$  DCT coefficients. Therefore, an experiment that investigates a ratio of the amount of enhancement codes to that of JPEG bit stream gives a fundamental property of the steganographic data embedding system when the quality factors of

both lower and higher frequency DCT coefficients are changed. The ratio of the amount of enhancement codes to JPEG bit stream is measured using a combination of  $QF_1, QF_2 = 40, 45, 50, 55, \dots, 90, 95$  with step of 5.

Six test images used in the experiment is described in Table 1 and Figure 10. L1, L2, and L3 are comparatively low resolution images, while H1, H2, H3 are comparatively high resolution images. The image L1 is SIDBA image, and the images L2 and L3 are obtained from [1] and clipped away to obtain center regions. The images H1, H2, and H3 are all from [2] and clipped away to obtain  $2048 \times 2048$  region.

Table 1 Test images.

Name	Pixel resolution	Note
L1	W512 × H512	lena
L2	W672 × H544	barbara
L3	W672 × H544	goldhill
H1	W2048 × H2048	p1rgb in SHIPP
H2	W2048 × H2048	p2rgb in SHIPP
H3	W2048 × H2048	p3rgb in SHIPP

## 4. EXPERIMENT RESULTS

### 4.1 Experiment phase I

#### • Experiment conditions

1. No scanning is performed for higher frequency DCT coefficients (i.e., scan = 0).
2. The chrominance formats are 4:4:4, 4:2:2, and 4:1:1.
3. 12  $QF_1$  are selected as 40, 45, ..., 90, 95 with step of 5.

#### • Measured items

1.  $\text{SNR}_{\text{lowpass}}$  that is measured as a SNR of low-pass filtered original-size JPEG coded image (scan = 0) for various  $QF_1$  values against original pixel resolution image.
2.  $\text{SNR}_{\text{lowres}}$  that is measured as a SNR of reduced-size JPEG coded image for various  $QF_1$  values against the output of  $16 \times 16$  DCT/ $8 \times 8$  IDCT filter bank system.
3. Compression ratio of reduced-size JPEG encoded image.

#### • Measured results

The measured results of  $\text{SNR}_{\text{lowpass}}$  and  $\text{SNR}_{\text{lowres}}$  are shown in Figures 11 and 12. The compression ratios

for images L1, L2, and L3 are lower than that for images H1, H2, and H3. These results mean that the images L1, L2, and L3 have more high frequency components than the images H1, H2, and H3. Specifically, as shown in Figure 11, images L1, L2, and L3 have low  $\text{SNR}_{\text{lowpass}}$ , so that the large aliasing effect is expected by the low pass filtering with  $16 \times 16$ -point DCT/ $8 \times 8$ -point IDCT system. On the other hand, images H1, H2, and H3 have comparatively small high frequency components, and, of these, the high frequency component of image H1 is extremely low. A simple subjective experiment shows that some image degradations are detected for L1 with  $QF_1 < 90$  when the image is magnified on a 23-inch HD LCD monitor.

#### 4.2 Experiment phase II

- Experiment conditions

1. 8 scanning modes are employed (scan = 1, 2, ..., 8).
2. The chrominance formats are 4:4:4, 4:2:2, and 4:1:1.
3. 12  $QF_2$  are selected as 40, 45, ..., 90, 95 with step of 5.
4. The default step sizes for higher frequency DCT coefficients are all set to 99.

- Measured items

Average, maximum, and minimum values of enhancement codes per block ( $16 \times 16$  region) in bits for various combinations of scan = 1, 2, ..., 8,  $QF_2 = 40, 45, 50, 55, \dots, 90, 95$  with step of 5, and three chrominance formats.

- Measured results

The average enhancement code length per block ( $16 \times 16$  region) for luminance component of images L1 and H2 is shown in Figure 13. For the 6 images used in the experiment, the minimum enhancement code lengths for luminance Y component and chrominance UV components are 4 and 2 bits, respectively. This means these images have at least one block that the entire quantized high frequency DCT coefficient is zero. In case that the quality factor for the higher frequency DCT coefficients,  $QF_2$ , is smaller than 50, the enhancement code lengths per block for chrominance components are mostly 2 bits in both average and maximum values, therefore it can be concluded that the higher frequency for chrominance compo-

nents scarcely contribute to the image enhancement.

For comparatively low resolution images L1, L2, and L3, the enhancement code length per block for luminance component is around 100 bits even though the quality factor,  $QF_2$ , is small, when entire frequency components are used for image enhancement (i.e., scan = 8). The  $8 \times 8$  DCT coefficients utilized to embed the enhancement codes is at most 64 even if they contain no zero-value DCT coefficients (in general, it is known from studies on watermarking and steganography [6] that an embedding into zero-value DCT coefficient leads to a large image degradation), so that, for example, a data embedding into at least 2 LSBs should be considered for 100-bit enhancement codes. Because this data embedding degrades the SNR of lower frequency DCT coefficients, the quality factor for the lower frequency DCT coefficients,  $QF_1$ , needs to be sufficiently large in order to keep the visual image quality unchanged even if such amount of enhancement codes are embedded. Another approach for alleviating this problem is to decrease the number of scans for high frequency DCT coefficients. In this case, however, it will not be preferable for images that have large high frequency components, as these components to be recovered are restricted. How to balance the magnitude of the quality factors,  $QF_1$  and  $QF_2$ , in terms of overall visual image quality is a future work.

On the other hand, for the images H1, H2, and H3, which have higher resolution than the images L1, L2, and L3, the enhancement code length for the luminance component is less than 100 bits when the quality factor for the high frequency DCT coefficients,  $QF_2$ , is relatively small, so that the SNR degradation with the LSB embedding is expected to be small in this case.

#### 4.3 Experiment phase III

- Experiment conditions

1. 8 scanning modes are employed (scan = 1, 2, ..., 8).
2. The chrominance formats are 4:4:4, 4:2:2, and 4:1:1.
3. 12  $QF_1$  and 12  $QF_2$  are selected as 40, 45, ..., 90, 95 with step of 5.
4. The default step sizes for higher frequency DCT coefficients are all set to 99.

- Measured items

A rate of the amount of enhancement codes against that of JPEG bit stream is measured for various combinations of  $QF_1$  and  $QF_2$ .

- Measured results

The rate in percent for images L1 and H2 are shown in Figure 14. As observed in the experiment phase II, it is obvious that the images L1, L2, and L3 have greater high frequency components than the images H1, H2, and H3. Specifically, the image L2 includes much high frequency in textures of the cloth. Moreover, the image H1 has very small high frequency components, while the image H2 has largest high frequency components among images H1, H2, H3, because H2 includes thin ropes in the image. It is concluded that the rate of the amount of enhancement codes against that of JPEG bit stream can be restricted within 10 % when a combination of higher  $QF_1$  and lower  $QF_2$  is used. The enhancement codes shown here include the codes for two chrominance components, so that the rate slightly decreases by ignoring these codes.

## 5. CONCLUSION

In this paper, we proposed a new image enhancement method with steganographic data embedding, and measured fundamental property of the method using various types of images. Although the SNRs in practice will decrease compared to the results obtained here because this consideration does not include the embedding of enhancement data in the LSBs of low frequency DCT coefficients, the property of the amount of the enhancement codes against various quality factor conditions can be obtained.

The experiments performed in section 4 consist phases I, II, and III, and the following results are obtained: Relatively high quality factor is needed for reconstruct original-size low-passed JPEG compressed image using DCT/IDCT system without entire high frequency components from the experiment phase I. From the experiment phase II, the amount of enhancement codes for luminance component is much larger than those for chrominance components.

Moreover, in order to embed the enhancement codes into the LSBs of low frequency DCT coefficients, it should be considered that at least 2 LSBs are used for that embedding. The rate of the amount of enhancement codes against that of JPEG bit stream can be restricted within about 10 % using an appropriate combination of quality factors for quantization of lower and higher frequency DCT coefficients from the experiment phase III.

The most important problems to implement the proposed method are how to embed the enhancement codes into the LSBs of  $8 \times 8$  DCT coefficients and how to balance the quality factors of lower and higher frequency DCT coefficients. These issues must be solved through subjective image quality tests, though the subjective evaluation depends on many viewing conditions, such as monitor size, magnification ratio, and so on. For this reason, we decided to study the problem of image quality assessment in conjunction with the embedding method for the enhancement data.

Our future topics are to study how to embed the enhancement data and how to balance the quality factors based on subjective evaluation.

## REFERENCES

- [1] H. Ogawa, "What can we see behind sampling theorems?", IEICE Tech. Report, CAS2007-124, pp.91-96, Mar. 2008.
- [2] S. Sugimoto and M. Okutomi, "Super resolution by image processing," Journal of the Robotic Society of Japan, Vol.23, No.3, pp.305-309, Apr. 2005.
- [3] A. Katsaggelos, R. Molina, and J. Mateos, Super Resolution of Images and Video: Chapter 2 Bayesian formulation of super-resolution image reconstruction, pp.13-17, Morgan & Claypool, 2007.
- [4] <http://www.hlevkin.com/TestImages/classic.htm>.
- [5] Standard High Precision Picture data (SHIP), IEEEJ, Apr. 1997.
- [6] I. Cox, M. Miller, J. Bloom, J. Fridrich, and T. Kalker, Digital Watermarking and Steganography, 2<sup>nd</sup> Ed., Morgan Kaufmann, 2008.

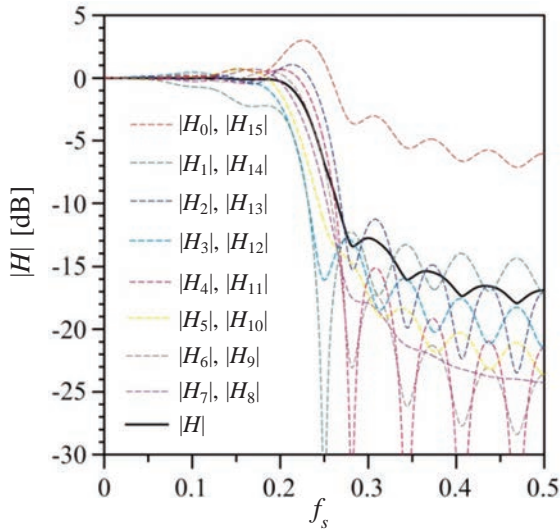


Fig. 4 Frequency response  $|H_n|$  and  $|H|$  of DCT/IDCT system with zero high frequency. ( $N = 16, L = 8$ )

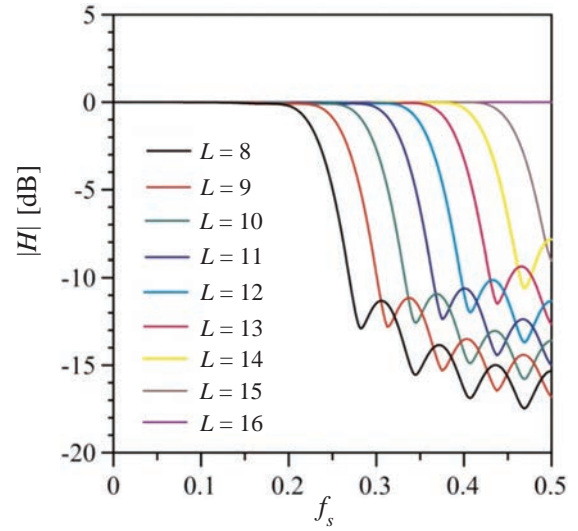


Fig. 8 Frequency response  $|H|$  of DCT/IDCT system with discarding high frequency. ( $N = 16, L = 8, \dots, 16$ )

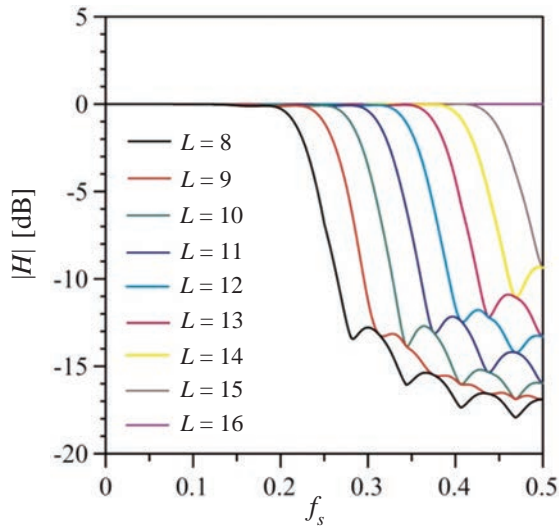


Fig. 5 Frequency response  $|H|$  of DCT/IDCT system with zero high frequency. ( $N = 16, L = 8, \dots, 16$ )

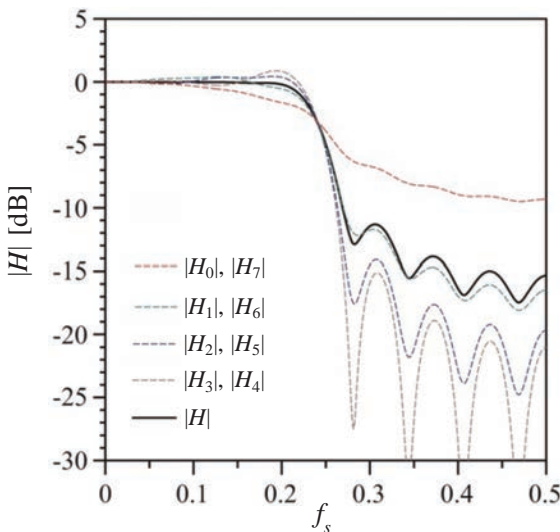


Fig. 7 Frequency response  $|H_n|$  and  $|H|$  of DCT/IDCT system with discarding high frequency. ( $N = 16, L = 8$ )



Fig. 10 Test images.

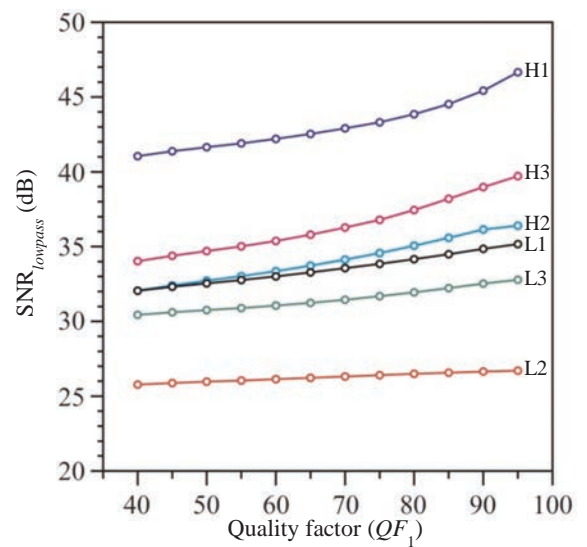


Fig. 11  $SNR_{lowpass}$  vs. quality factor in lower frequency.

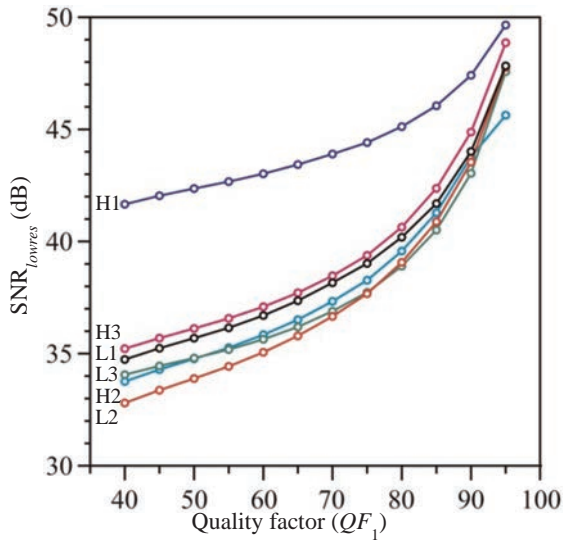
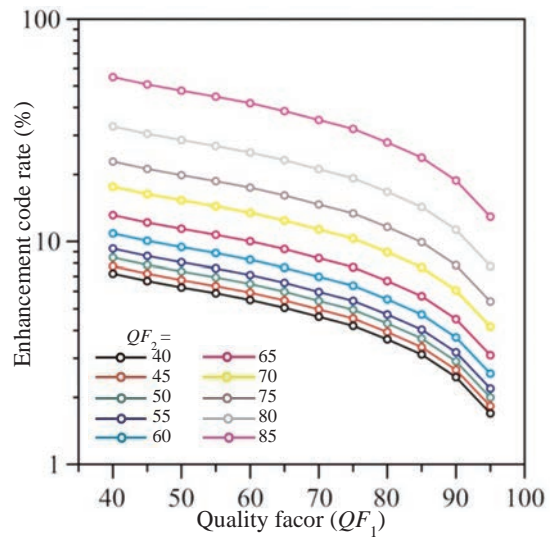
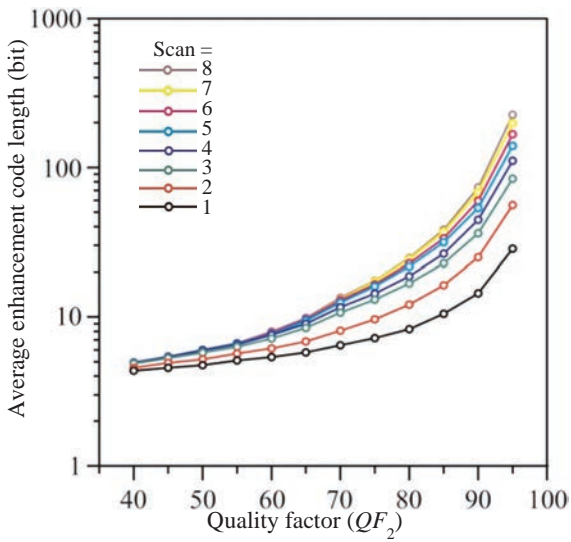


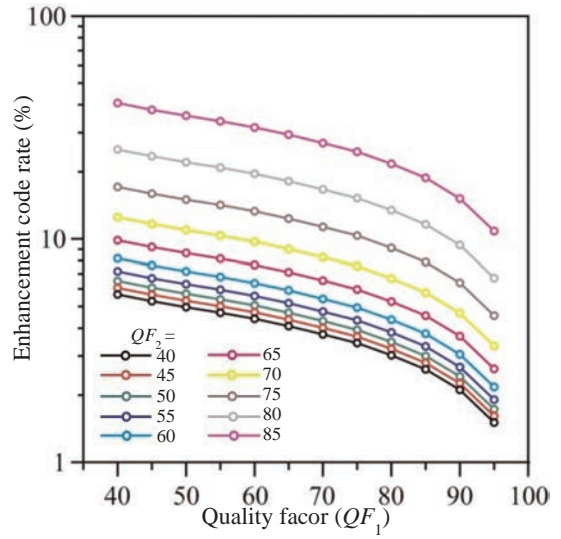
Fig. 12 SNR<sub>lowres</sub> vs. quality factor in lower frequency.



(a) image L1

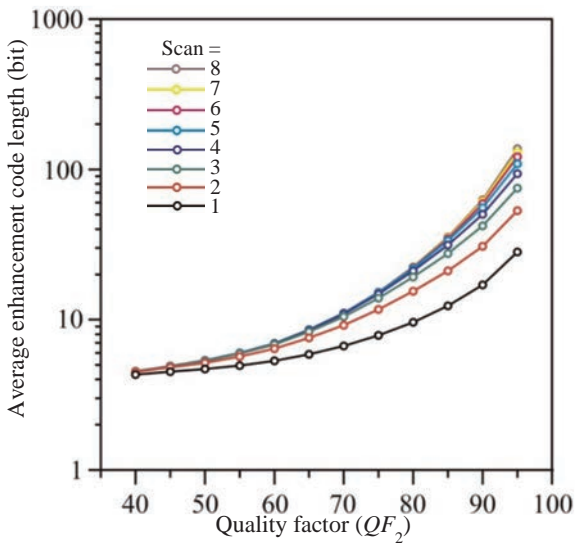


(a) image L1



(b) image H2

Fig. 14 Ratio of enhancement codes to JPEG codes.



(b) image H2

Fig. 13 Average enhancement code length per block.

